Supplementary Information

The nickel-sirohydrochlorin formation mechanism of the ancestral class II chelatase CfbA in coenzyme F430 biosynthesis

Takashi Fujishiro,* Shoko Ogawa

Department of Biochemistry and Molecular Biology, Graduate School of Science and Engineering, Saitama University, Saitama, Japan

***Corresponding author:**

T. Fujishiro, Department of Biochemistry and Molecular Biology,

Graduate School of Science and Engineering, Saitama University,

Shimo-Okubo 255, Sakura-ku, Saitama 338-8570, Japan

Tel: +81-48-858-9293

E-mail: tfujishiro@mail.saitama-u.ac.jp

Experimental details

Materials

All chemicals, except for those described below, were purchased from Sigma-Aldrich (St. Louis, MO, USA), Nacalai Tesque (Kyoto, Japan), Wako Pure Chemicals (Osaka, Japan), or Tokyo Chemical Industry Co., Ltd. (Tokyo, Japan) and used without further purifications. Porphobilinogen (PBG) was purchased from Frontier Scientific, Inc (Logan, UT, USA). Isopropyl-β-D-thiogalactopyranoside (IPTG) was purchased from BLD Pharmatech Inc. (Shanghai, China). The genomes of *Methanocaldococcus jannaschii* and *Methanosarcina barkeri* were obtained from RIKEN BRC through the National BioResource Project of the MEXT/AMED, Japan.

Bioinformatics

Primary amino acid sequence alignment was performed using Clustal omega[1] with the sequences of nickel-chelatase CfbA from methanogenic archaea, cobalt-chelatase $CbiX^S$ from archaea with no coenzyme F430, and ferrochelatase SirB from *Bacillus subtilis* (Fig. S4). The sequence alignment figure was constructed using ESPript3.[2] A phylogenetic tree was created with MEGA 7.0[3], utilizing the maximum-likelihood method with the JTT model, 1000 bootstrap replicates, and complete gap deletion. SirB ferrochelatase from *B. subtilis* was used as an outgroup (Fig. S5).

Construction of expression plasmids of *M. jannaschii* CfbA and its variants

The *cfbA* (MJ0970-tagged gene) was amplified from the genome of *M. jannaschii* through polymerase chain reaction (PCR) using the NcoI_MjCfbA-F and SalI_MjCfbA-R primers (Table S1). The amplified *cfbA* was incorporated into the pCDFDuet-1 vector (Novagen, Merck Millipore, Burlington, MA, USA) at the *Nco*I and *Sal*I restriction sites, yielding the pCDFDuet-*cfbA* plasmid. The *M. jannaschii* CfbA H9A variant was generated using the same protocol, except for the mutagenic forward primer NcoI_MjCfbA_H9A-F (Table S1). Site-directed mutagenesis was performed to create the expression constructs for CfbA E42A and H75A variants. This involved inverse PCR using the pCDFDuet-*cfbA* plasmid as a template and the primers MjCfbA_E42A-F, MjCfbA_E42A-R, MjCfbA_H75A-F, MjCfbA_H75A-R (Table S1).

Construction of chimeric CfbA expression plasmid

A chimeric CfbA was created by substituting the His-rich region with the non-His-rich region of *M. barkeri* CfbA. First, the DNA sequence corresponding to the non-His-rich region of *M. barkeri* CbfA was amplified using the genome of *M. barkeri* as a template and the primers No_His_region_MbCfbA-F and No_His_region_MbCfbA-R (Table S1). Second, the His-rich region-encoding polynucleotides in pCDFDuet-*cfbA* was amplified via inverse PCR with the primers No_His_rich_MjCfbA_pCDF-F and No_His_rich_MjCfbA_pCDF-R. After amplification of these two gene segments, gene assembly was performed using NEB builder HiFi DNA Assembly Master Mix (New England Biolabs, Inc., Ipswich, MA, USA). The constructed plasmid was sequenced to confirm the substitution in the chimeric *cfbA*. The resulting expression plasmid for the chimeric CfbA was annotated as pCDFDuet-*chimcfbA.* The gene and amino acid sequences of the resulting chimeric *M. jannaschii* CfbA are provided as below, with a substituted His-rich region underlined.

(DNA sequence’

5'-

ATGGAAGCGTTGGTTTTAGTAGGACATGGGAGTAGATTACCCTACAGCAAAGAGCTTCTGGTAAAGTT

AGCTGAGAAAGTTAAAGAGAGAAATTTATTCCCAATAGTTGAAATTGGTTTGATGGAGTTTAGTGAGC

CAACAATACCTCAAGCAGTTAAAAAAGCTATAGAACAAGGGGCTAAAAGAATCATTGTTGTTCCTGTTT

TCTTAGCTCATGGAATTCATACAACAAGAGATATTCCAAGGTTATTGGGGTTGGACGAAAATGGCTGTG

GTACCTTGGAAATTGACGGAAAAACCGTTGAAATTATATATAGAGAACCTATTGGAGCAGATGATAGAA

TTGTTGATATAATTATCGATAGAGCATTTGGAAGATA’-3'

(Amino acid sequence)

MEALVLVGHGSRLPYSKELLVKLAEKVKERNLFPIVEIGLMEFSEPTIPQAVKKAIEQGAKRIIVVPVFLAHGI

HTTRDIPRLLGLDENGCGTLEIDGKTVEIIYREPIGADDRIVDIIIDRAFGR

Expression of *M. jannaschii* wild-type, chimeric, and variant CfbA enzymes

The *Escherichia coli* C41(DE3) cells transformed with the expression plasmids of wild-type, chimeric and variant CfbA enzymes were cultivated at 37°C for 4 h in Luria-Bertani (LB) medium supplemented with 50 µg mL^{-1} spectinomycin. At an optical density of OD_{600} = 1.0, IPTG was added to the culture to a final concentration of 1 mM to induce the expression of CfbA. The cells were further cultured at 20°C for 20 h, harvested by centrifugation at 4°C at 9,000 *g* for 20 min and frozen in liquid nitrogen. The frozen cells were stored at -80 °C until further use. Attempts to express the CfbA variants (H9A, E42A, and H75A) using the same procedure for wild-type and chimeric CfbA were unsuccessful.

Purification of *M. jannaschii* wild-type CfbA

All purification steps were performed on ice or at 4°C. The frozen cells were first resuspended in buffer A (50 mM Tris-HCl buffer, pH 7.8, 500 mM KCl, and 1 mM dithiothreitol (DTT)), disrupted on ice by sonication, and then centrifuged at 4°C at 20,000 *g* for 40 min. The supernatant prepared by centrifugation of the sonicated cells was then loaded onto a HisTrap FF crude column (GE Healthcare Life Science, Chicago, IL, USA), equilibrated with buffer A. CfbA bound to the HisTrap FF crude column using its naturally occurring His-rich region. The column was then washed with buffer A and the bound CfbA was eluted with buffer B (50 mM Tris-HCl, pH 7.8, 500 mM KCl, 250 mM imidazole, and 1 mM DTT). The eluted CfbA fraction was concentrated to 5 mL using an Amicon Ultra-15 (Merck KGaA, Darmstadt, Germany). The concentrated CfbA fractions were loaded onto a Sephacryl S-200 16/60 gel filtration column (GE Healthcare Life Sciences) equilibrated with buffer C (50 mM Tris-HCl, pH 7.8, 150 mM NaCl, and 1 mM DTT). The CfbA eluted as a homodimer, and the fractions were pooled for further use.

Purification of the chimeric CfbA

Purification of the chimeric CfbA was performed as follows: The harvested *E. coli* C41(DE3) cells were resuspended in buffer D (50 mM Tris-HCl, pH 7.8, 50 mM NaCl, 1 mM DTT) and disrupted by sonication on ice. The supernatant collected by centrifugation was heated at 80°C for 20 min. The heated solution was further centrifuged at 4°C at 20,000 *g* for 40 min to remove the precipitate. The resulting supernatant was subsequently loaded onto a HiTrap Q HP column (GE Healthcare Life Sciences), equilibrated with buffer D. The column was washed with buffer D and the chimeric CfbA was eluted with a stepwise gradient of sodium chloride ranging from 0 M to 1 M using buffer E (50 mM Tris-HCl, pH 7.8, 1 M NaCl, 1 mM DTT). The pooled chimeric CfbA fractions were concentrated and then loaded onto a Sephacryl S-200 16/60 gel filtration column equilibrated with buffer C. The chimeric CfbA also eluted as a homodimer, and the fractions were pooled for further use.

Metal content analysis of purified *M. jannaschii* wild-type and chimeric CfbA

The presence of transition metal ions in the purified wild-type CfbA fractions was analyzed using inductively coupled plasma-atomic emission spectrometry (ICP-AES) with an Optima 5300 DV system (PerkinElmer Inc., Waltham, MA, USA). Samples were prepared by heating CfbA in 3% (v/v) aqueous HNO_3 at 100°C for 10 min, and then centrifuged at 4°C at 15,000 *g* for 10 min to obtain the supernatant for ICP-AES. The standard nickel solution (Nacalai Tesque, Kyoto, Japan) was used to plot calibration curves. It should be noted that there were no metals co-purified with wild-type and chimeric CfbA.

Preparation of HemC, HemD, SirA, and SirC

HemC (porphobilinogen deaminase, BSU28150), HemD (uroporphyrinogen-III synthase, BSU28140), SirA (uroporphyrinogen-III C-methyltransferase, BSU15610; SirA is also annotated as SumT) from *B. subtilis,* as well as SirC (precorrin-2 dehydrogenase, MSBRM_0432) from *M. barkeri* were expressed and purified as *E. coli* recombinant proteins with a His-tag for use in the enzymatic preparation of sirohydrochlorin (SHC) as described previously.[4]

For the construction of HemC, HemD, and SirA expression plasmids, the corresponding *hemC*, *hemD,* and *sirA* were amplified via PCR using the *B. subtilis* genome as a template and the corresponding primers (Table S2). The amplified *hemC*, *hemD,* and *sirA* were

then ligated to pET21d vector (Novagen) at *Nco*I/*Xho*I restriction sites, yielding pET21d-*hemC*, pET21d-*hemD*, and pET21d-*sirA* expression vectors, respectively. The *sirC* from *M. barkeri* was also amplified via PCR using the *M. barkeri* genome as a template with corresponding primers (Table S2). The amplified *sirC* was ligated to the pACYCDuet vector (Novagen) at *Bam*HI/*Sal*I restriction sites, yielding the pACYC-*sirC* expression vector.

The expression vectors for HemC, HemD, SirA, and SirC were used for transformation of *E. coli* C41(DE3). Then, the transformed *E. coli* C41(DE3) cells were cultivated at 37°C for 4 h in LB medium supplemented with 50 µg mL^{-1} ampicillin to express HemC, HemD, and SirA and with 25 µg mL^{-1} chloramphenicol to express SirC. When OD_{600} reached 0.8–1.0, the protein expression was induced by the addition of 1 mM IPTG, and the cells were further cultured at 20°C for 20 h. The cells were harvested by centrifugation at 4°C at 9,000 *g* for 20 min. The purification of HemC, HemD, SirA, and SirC was performed using the wild-type CfbA purification protocol described above. The purification of HemC, HemD, SirA, and SirC was confirmed via SDS-PAGE (Fig. S8).

Preparation of SHC and Ni-SHC

SHC was prepared as described previously,[4] with some modifications. Briefly, a reaction mixture for one-pot synthesis of SHC was prepared using 0.075 mM of porphobilinogen (PBG), 0.175 mM of *S*-adenosyl-L-methionine (SAM), 0.2 mM of nicotinamide adenine dinucleotide phosphate ($NADP^+$), 4 mM of $MgCl_2$, 2.5 µM of HemC, 2 µM of HemD, 4.2 µM of SirA, and 16 µM of SirC in 50 mM Tris-HCl, pH 8.0, under dark conditions in a Coy chamber (N_2/H_2 =95/5), at 37°C for 24 h. The reaction mixture was then anaerobically passed through a HiTrap desalting column (GE Healthcare Life Sciences), equilibrated with deionized water, to collect the fractions containing SHC. Then, the pooled SHC fractions were loaded onto a HiTrap DEAE FF column (GE Healthcare Life Sciences) equilibrated with deionized water. After washing the column with 0.2 M NaCl, bound SHC was eluted with a linear gradient of NaCl ranging from 0.2 to 1 M. The SHC fractions were pooled and evaporated in vacuo and SHC was collected. MALDI-TOF-MS of SHC was measured using an Autoflex III-2S (Bruker Corp., Billerica, MA, USA) with α-cyano-4-hydroxycinnamic acid as a matrix (Fig. S9).

For the preparation of Ni-SHC, nickel-chelatase reaction catalyzed by CfbA was anaerobically performed in 7.5 mL of reaction mixture composed of 0.038 mM SHC, 1.3 mM $NiCl_2$, 10 µM CfbA, 150 mM NaCl, 1 mM tris(2-carboxyethyl)phosphate (TCEP) in 50 mM Tris-HCl, pH 7.8, at 37°C for 16 h in the dark in a Coy chamber (N_2/H_2 = 95/5). The reaction mixture was then passed through a HiTrap desalting column (GE Healthcare Life Sciences) to collect the fractions containing Ni-SHC. Then the pooled Ni-SHC-containing fractions were loaded onto the HiTrap DEAE FF column (GE Healthcare Life Sciences) equilibrated with deionized water. After washing the column with 0.2 M NaCl, bound Ni-SHC was eluted in a stepwise gradient of NaCl ranging from 0.2 to 1 M. Finally, the pooled Ni-SHC fractions were evaporated in vacuo, which yielded a Ni-SHC precipitate. MALDI-TOF-MS of Ni-SHC was measured with α-cyano-4-hydroxycinnamic acid as a matrix (Fig. S9).

The *in vitro* CfbA activity assay with Ni^{2+} and Co^{2+}

The assay mixture was composed of 0.4 µM CfbA and 0.2 µM SHC in 50 mM Tris-HCl buffer, pH 8.0, in an anaerobic Coy chamber under N_2/H_2 = 95/5. The reaction was initiated by the addition of 5 µM $NiCl_2$ or $CoCl_2$ to the mixture of SHC and CfbA in a quartz cuvette having a 1-cm cell path. The change in UV-visible absorption at 408 nm was recorded on a NanoPhotometer C40 UV-visible spectrophotometer (Implen GmbH, Munich, Germany). The specific activities were determined by calculating the pseudo-first-order kinetic constant (k_{app}) using a non-linear least squares data-fitting to time-course changes of absorbance at 408 nm using Igor Pro 8.0 software (WaveMetrics, Inc., Lake Oswego, OR, USA) (Figs. S6, S7).

Crystallization of *M. jannaschii* wild-type and chimeric CfbA

The purified *M. jannaschii* wild-type and chimeric CfbA proteins were concentrated to 14–18 mg mL^{-1} and 16 mg mL^{-1}, respectively, in a buffer containing 50 mM Tris-HCl, pH 7.8, 150 mM NaCl, and 1 mM DTT. Crystallization was carried out using the sitting drop vapor diffusion method at 20°C, mixing 1 µL of the purified protein with an equivalent volume of the reservoir solution (Table S3). Crystals of the wild-type and chimeric protein appeared in two weeks and five months, respectively.

Preparation of crystals of CfbA in complex with Ni^{2+} and Co^{2+}

Apo-CfbA and ligand-bound CfbA crystals (Table S3) were soaked with the ligand of interest. Ni^{2+}-bound CfbA crystals were obtained by soaking apo-CfbA crystals with 0.1 mM $NiCl_2$ at 20°C for 1 h, followed by soaking in 0.5 mM $NiCl_2$ at 20°C for 30 min. The Co^{2+}-bound crystals of CfbA resulted from the soaking of CfbA with 1 mM $CoCl_2$ at 20°C for 15 h. By contrast, the crystals of Co^{2+}- and formate-bound form of CfbA was unexpectedly obtained as follows: apo-CfbA crystals were first soaked with 1 mM uroporphyrin I (Sigma-Aldrich, St. Louis, MO, USA) for 2 days, followed by soaking with 0.5 mM $CoCl_2$ for 10 min. Uroporphyrin I was, however, not observed in the solved CfbA structure.

Preparation of CfbA crystals with SHC and Ni-SHC

Crystals of SHC- and Ni-SHC-bound forms of CfbA were prepared by soaking apo-CfbA crystals with 4.0 mM SHC and 3.7 mM Ni-SHC, respectively, at 20°C for 15 h under anaerobic conditions.

Preparing crystals of Ni^{2+}-SHC-His intermediate and Co-SHC-bound form of CfbA

To trap a reaction intermediate, we further soaked the SHC-soaked CfbA crystals described above in Ni^{2+} or Co^{2+}. For Ni^{2+}-soaking, the SHC-soaked CfbA crystals were soaked in 1 mM $NiCl_2$ at 20°C for 6.5 h and flash-frozen in liquid nitrogen. However, for Co^{2+}-soaking, the crystals yielded Co-SHC bound to CfbA rather than an intermediate. For this, the SHC-soaked crystals were further soaked in 1 mM $CoCl_2$ at 20°C for 1 h, followed by flash-freezing in liquid nitrogen.

X-ray crystallographic analysis

X-ray diffraction data of the CfbA crystals were collected at 100 K on the Photon factory (PF) BL-17A and PF AR-NW12A beamlines (Tsukuba, Japan), and SPring-8 BL44XU beamline (Hyogo, Japan). All data sets were processed using XDS,[5] except for the apo-CfbA, which was processed using iMOSFLM.[6] The structures were solved using molecular replacement with Molrep[7] or Phaser[8] using *Archaeoglobus fulgidus* CbiX^S (PDB ID: 2XWS)[9] as the search model. Models were built using Coot[10] and refined using Refmac5[11] and Phenix[12]. Model coordinates and restraints

of the ligands SHC, Co-SHC, and Ni-SHC were generated using Sketcher in CCP4[13] and eLBOW in Phenix.[14]

Translation-liberation-screw-rotation refinement was also performed for the data sets of $P2_12_12_1$ apo-CfbA, Ni^{2+}-bound CfbA, Ni-SHC-bound CfbA, and Co-SHC-bound CfbA at the final stages of modeling with TLSMD.[15] The final structural models were validated using MolProbity.[16] Figures containing crystal structures were created using open-source PyMOL (version 1.7, Schrödinger, LLC). The anomalous difference density maps for nickel and cobalt were calculated using the data sets collected at peak wavelengths of nickel and cobalt, respectively. Data collection, refinement statistics, and PDB IDs of the deposited models are listed in Table S4.

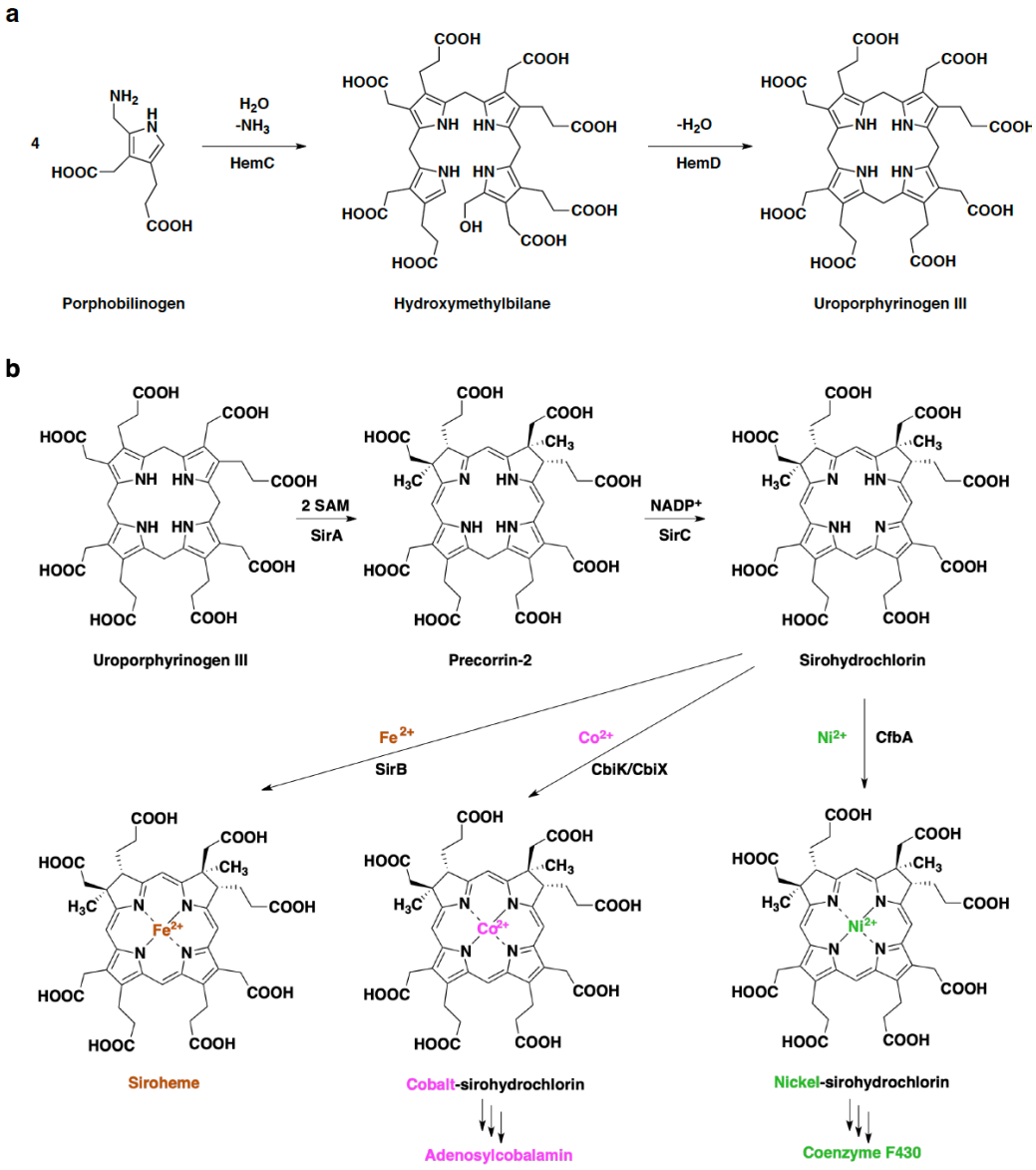

Fig. S1. Biosynthesis of coenzyme F430 and its related compounds. (a) Biosynthetic pathways of uroporphyrinogen III. (b) Biosynthetic pathways of siroheme, adenosylcobalamin, and coenzyme F430 via sirohydrochlorin (SHC). SirB, CbiK/CbiX, and CfbA are ferrochelatase, cobalt chelatase, and nickel chelatase, respectively.

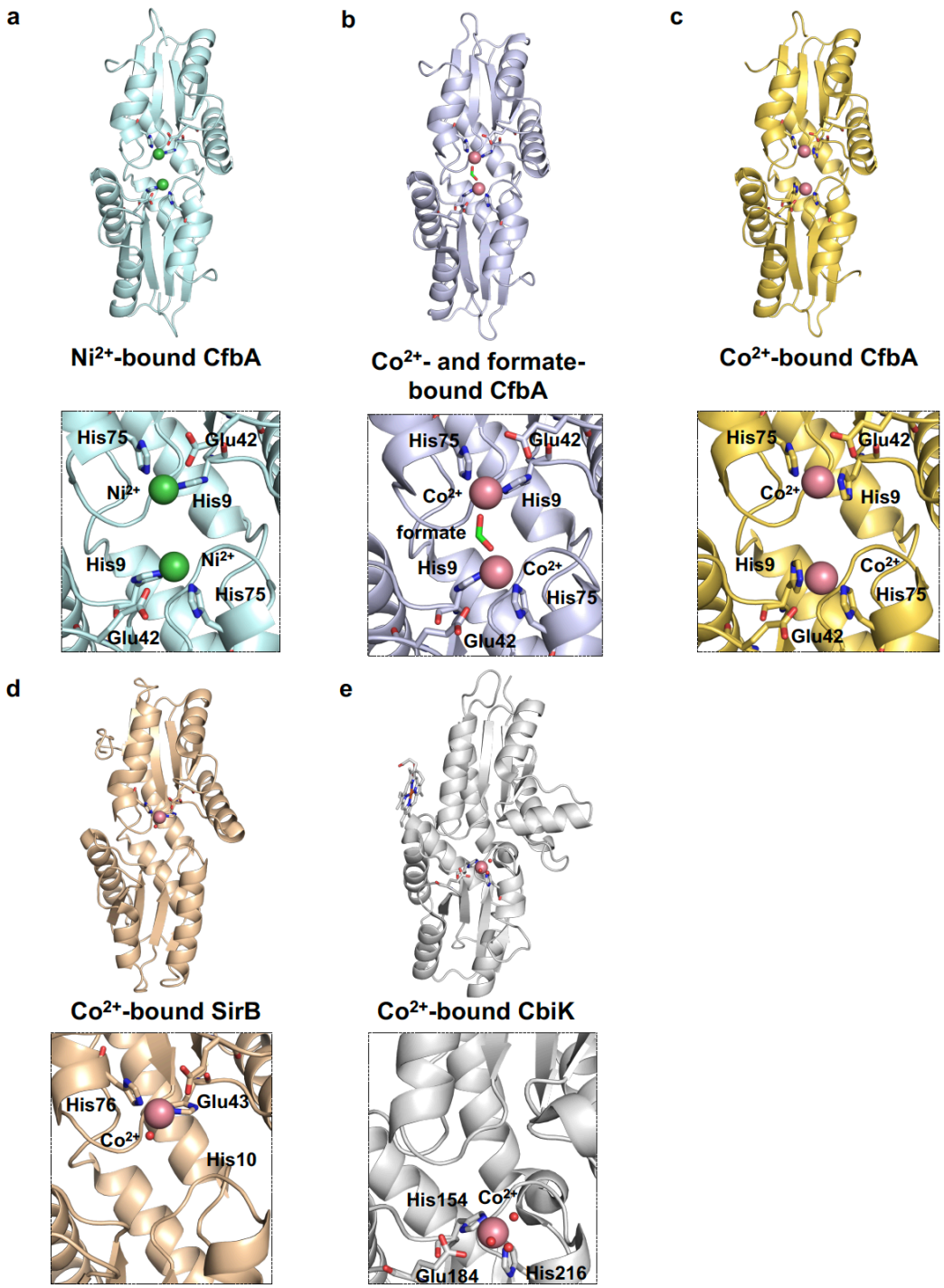

Fig. S2. Overall structures and active sites of type II chelatases with metal ions. (a) Ni^{2+}-bound CfbA (PDB ID: 6M27, this study). (b) Co^{2+}- and formate-bound CfbA (PDB ID: 6M29, this study). (c) Co^{2+}-bound CfbA (PDB ID: 6M28, this study). (d) Co^{2+}-bound SirB (PDB ID: 5ZT7) [17]. (e) Co^{2+}-bound CbiK (PDB ID: 2XVZ) [4]. Water molecules bound to metal ions are shown as small red spheres. Ni^{2+} is represented by green spheres and Co^{2+} by pink spheres. The side chains of conserved amino acids, formate and haem molecules are shown using sticks

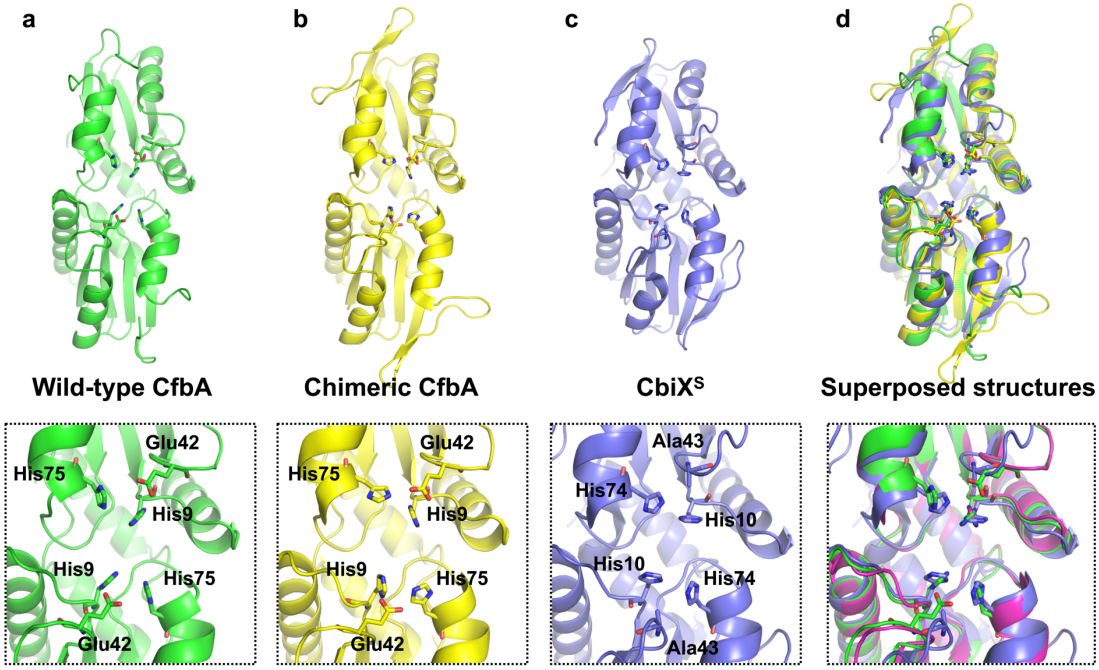

Fig. S3. Overall structures and active sites of CfbA and CbiX^S. (a) Wild-type CfbA (PDB ID: 6M25, this study). (b) Chimeric CfbA (PDB ID: 6M2A, this study). (c) CbiX^S from *Archaeoglobus fulgidus* (PDB ID: 2XWQ). (d) Superimposed structures of wild-type CfbA and chimeric CfbA, and CbiX^S. The side chains of conserved amino acids are shown as sticks.

```
                                          1         10        20        30        40        50        60
M_jannaschii_CfbA                 ..............MEALVLVGHGSRLPYSKELLVKLAEKVKERNLFPIVEIGLMEFSEPTIPQAVKKAIEQGAKRIIVV
M_igneus_CfbA                     ..............MEALVLVGHGSRLPYSKEVVEKIAEKIRAKNIYPIVEVGMMEFNEPTIPQAVKKAIEQGAKKIIVV
M_formicicus_CfbA                 ..............MEALVLVGHGSRLPYSKEIVEKIAEKIKAKNIYPIVEVGMMEFNEPTIPQAVKKAIEQGAKKIIVV
M_maripaludis_CfbA                ..............MEALVLVGHGSRLPHSKNVVTEVAEKIKARNIYDIVEVGMMEFNEPTIPEAIKKVIDAGAKKVIVT
M_thermolithotrophicus_CfbA       MKNHCKNITQRRHIMEALVLVGHGSRLPYSKETVYAIAEKIKEKGTYPIVEVGMMEFNEPTIPQAVKKVIEKGAKKVIVV
M_kandleri_CfbA                   ..............MVAVVLVGHGSRLPYSRQVVEKIAEYVEEMGDFETVEVGFMELCEPTVQEAVKKAAESGVDKIVVV
M_formicicum_CfbA                 .....MVTNSNSNSNVGIVLVGHGSRLPYGKDVLSQLAEIYRQ.ESDHPVEVGFMNMNKPSIPSSINKLAQMGVEKIVVT
M_stadtmanae_CfbA                 .....MDTNSNSKNDTGILLIGHGSRLPYNKEVISAIAEKYAQTKPDYNIEVGFMELAEPNIPTAFNKLKETGVNRIIVT
M_marburgensis_CfbA               .....MDSNSGQKTKIGVLLVGHGSRLPYGEEVINGIADIYRK.EVDHPVAVGFMNISRPSIPEAINELAAMGVEKIIVT
M_thermautotrophicus_CfbA         .....MDSNSNQKPKIGVLLVGHGSRLPYGEEVINGIADIYRQ.EADHPVAVGFMNMSRPSIPEAINELAAMGVEKIIVT
M_wolfeii_CfbA                    .....MDSNSNPEGKIGVLLVGHGSRLPYGEEVIKGIADIYRK.EADHPVAVGFMNISKPSIPEAINELAARGVEKIIVT
M_fervidus_CfbA                   .....MASNLDQKNDIAVLLVGHGSRLPYSKEVIMKLAEMYKE.RTDHLVDVAFMELAKPSIPETVNKLAKKGVRKIIVI
M_arvoryzae_CfbA                  .........ME.NQKFGLLVVGHGSMPYNKELIEDIAARIAKKMPDAVVRVGFMNMNKPTIKEGLDSFNGTGVRKIVVF
M_conradii_CfbA                   .........MEKSEKFGLLIVGHGSSQPYNKQLIQEVADKLSKKMPDAVTRIGFMNINKPSIKDALDSFVGTGVKKIVVF
M_labreanum_CfbA                  ...MTNQKHMSA...KGLLLVGHGSRLQYNKELITTTAEMMKESGGDYLIKSCFLEYSNPTVAEGLDLMRSEDLEILIVV
M_bourgensis_CfbA                 ..................MLLVGHGSKLPYNKELIETTAEFIAEKTDEYIVKPGFMSINAPTVEEQLDAFRTEDINMLVVV
M_liminatans_CfbA                 .........MAR...TGLLLVGHGSKLPYNKELIESTAALIASQHPEYLVRPGFMSMNEPSVDEALDAFKKDEIDLLIVV
M_petrolearia_CfbA                .........MPK...IGFLLVGHGSKKPYNKQLIDNTAKIIAGKEAGYIVKTGFMEFSEPTIPEALESFRGEDIEMLQVV
M_mobile_CfbA                     .........MSK...TGFLLVGHGSTKPYNKQLIENTAKLIAQKEKDYIVKCAFMENSTPSIPEIIETFRNEDIDKMLVV
M_limicola_CfbA                   .........MVK...KGFLLVGHGSKKPYNKQLIESTAAIISGKEDGYIVKSAFMENSSPTIQEMLEEFKKEEIDTLVVV
M_formicica_CfbA                  .........MSK...KGMLLVGHGSTMPYNQELVEKTAAMIQAKNNDFIVKCGFMNINKPTIRESMDAFRKEQIDALVVV
M_palustris_CfbA                  .........MSS...KGLLLVGHGSKLQYNKELILETGKMITGKSSEFMVKCGFMSMNEPSVEKMLEEFSHTAIDVLVVV
M_hungatei_CfbA                   .........MTK...TGILLVGHGSKKEYNKNLITKTAEIIAQKNPDYIVRCGFMEFNEPTIRESLDSFKQDEVDSIAVV
M_concilii_CfbA                   ..........MK..DVGILVLGHGSSLPFNKELVESLAQMIGKNNSSGPVRTAYLNMNQPDIPAGLKSFQGTGVKKIVAL
M_thermophila_CfbA                ..........ME..DIGLLVLGHGSTLPYNKALVEELAGMIKRKHP.GPVRTAYLNANDPKIPEGLMSFAGTNVRKIVAI
M_methylutens_CfbA                .........MSE..KIGILAIGHGSRLPYNKEVVSEIADTIAKKHPEYVVKVGFMENCGPSVDEGLASFEGTGVTKIAAV
M_evestigatum_CfbA                .........MSENSKLGILAIGHGSKLPYNKQVVTDIANRIADKHEDVVVRAGFMEKNEPTVEEALQSFEGTGISKIAAV
M_mahii_CfbA                      .........MSE..KIGILAIGHGSRLPYNKEVVTNIANTIAEKHPEYVIRTGFMENCGPSVQEAMKEFEGTGVTRIAAV
M_psychrophilus_CfbA              .........MTE..KMGILTIGHGSRLPYNNQVVSEIADMIAKKHPEYIVKSGFMEMSTPSVEEALLSFAGTGVTKIAAV
M_hollandica_CfbA                 .........MSE..KIGILAIGHGSRLPYNNQVVTEIAGMIAKKHPEYVVKAGFMEMSTPSVEEALLSFEGTHVSTIVAV
M_zhilinae_CfbA                   .........MTE..KIGILAIGHGSRLPYNKEVVTSIANNIAEKYENVVVRAGFMEHCGPSVEEALKAFDGTGVTKIVAV
M_acetivorans_CfbA                .........MTE..KLGILAIGHGSKLPYNKEVVSQIADYIAQKHSDVVVRAGFMENSEPTLEEAIAGFAGTGVTKIAAV
M_barkeri_CfbA                    .........MTE..KLGILAIGHGSKLPYNKEVVTQIADHIARKHSDVVVRAGFMENSEPTLGEAIEGFSGTGVTKIAAV
M_shengliensis_CfbA               ...MHGEFIMKR....GVLVLGHGSKLPYNREVVESVCSMLRQMRDDIMVVPAFMELCEPTIEDGLEELAKSGVSEVAVV
M_luminyensis_CfbA                .........MTN....GVLLIGHGSKLQYNKDLVVSTAEKMGKMNLG.PVAAAFMQLNTPTIKEGIKTLVGQGVDDIYIQ
Ca_M_intestinalis_CfbA            .........MKT....GVIVIGHGSKLDYNKKVVDFTAEKMKGMGLG.PVTPAYMQLNAPTIDEGMKWLVSQGVDTIFVQ
Ca_M_nitroreducens_CfbA           .......MIMSE..KIGILALGHGSKHPHNKDVVTGVAELIAKKYSNVVVRTGFMNMNSPTMKEGLDAFQGTGVSTIVAV
Ca_S_caldarius_CfbA               .......MRDMEKDKIALVLVGHGSVLAYNREMIEALANMIKERGVYDIVEHSFLQLNEPLLEDVLMGLASNGVGKIVVS
A_fulgidus_CbiXS                  .............MRRGLVIVGHGSQLNHYREVMELHRKRIEESGAFDEVKIAFAARKRRPMPD..EAIREMNCDIIYVV
G_ahangari_CbiXS                  .............MRKGLVIVGHGSQLPHYNRVMELHAERIRKFGIFDEVEIAFVARNRKPSPD..EAVRGMDCDVVYLV
S_islandicus_CbiXS                ..............MLGVLLVLHGSKIPEWKDVGIKYAEYLSRYFN..LVEFGFLEFNKPTLSEALSNLLAKGANKIVVV
A_sulfidivorans_CbiXS             ..............MIGVILVLHGSRIDEWKDVATQYKKLLENYFP..LVEYGFLEFNKPDLKEALQILVNKGANEIIAV
B_subtilis_SirB                   .............MKQAILYVGHGSRVKKAQQEAAAFLEGCKAHISVPVQEISFLELQEPTIETGFEACVKQGATHIAVV

                                  70        80        90
M_jannaschii_CfbA                 PVFLAHGIHTTRDIPRLLGLIEDN.....................................................
M_igneus_CfbA                     PVFLAHGNHTKRDIPRILGLIEDDGE...................................................
M_formicicus_CfbA                 PVFLAHGNHTKRDIPRILGLIEDDGE...................................................
M_maripaludis_CfbA                PVFLAPGNHTERDIPKILGIYEGDDD...................................................
M_thermolithotrophicus_CfbA       PVFLAHGNHTKRDIPKILGVYDGE.....................................................
M_kandleri_CfbA                   PVFLAHGVHTKRDIPKMLGLEPEWD....................................................
M_formicicum_CfbA                 PVFLAPGVHTTEDIPRILGLG........................................................
M_stadtmanae_CfbA                 PIFLAHGMHTKRDIPTILGLEPEVKEEP.................................................
M_marburgensis_CfbA               PVFLAHGVHTKHDIPHILGLD........................................................
M_thermautotrophicus_CfbA         PVFLAHGVHTKHDIPHILGLD........................................................
M_wolfeii_CfbA                    PVFLAHGVHTKHDIPHILGID........................................................
M_fervidus_CfbA                   PVFLAHGVHTKHDIPHILGLK........................................................
M_arvoryzae_CfbA                  PLFLAKGVHIKEDIPNLIGLK........................................................
M_conradii_CfbA                   PLFLAKGVHTTEDVPGLIGLG........................................................
M_labreanum_CfbA                  PLFLAKGIHILRDIPKILGLEA.......................................................
M_bourgensis_CfbA                 PLFLARGVHIDQDIPGILGLPE.......................................................
M_liminatans_CfbA                 PLFLAKGVHILQDIPELLGLPE.......................................................
M_petrolearia_CfbA                PLFLARGMHIDKDIPEILGIEE.......................................................
M_mobile_CfbA                     PLFLARGVHIDVDIPEILGIPE.......................................................
M_limicola_CfbA                   PLFLARGIHIDKDIPEILGIEE.......................................................
M_formicica_CfbA                  PLFLAKGVHIEKDIPGEIGLPE.......................................................
M_palustris_CfbA                  PLFLAKGVHIEKDIPSLLGLPE.......................................................
M_hungatei_CfbA                   PLFLARGVHIDEDIPGILGLAP.......................................................
M_concilii_CfbA                   PLFLAHGVHTRQDIPHELGVDP.......................................................
M_thermophila_CfbA                PLFLAAGVHTLEDIPRELGIPK.......................................................
M_methylutens_CfbA                PVFLASGVHITEDIPEILKLDA.......................................................
M_evestigatum_CfbA                PVFLASGVHITQDIPEILGIDP.......................................................
M_mahii_CfbA                      PVFLASGIHITEDIPEILKLDP.......................................................
M_psychrophilus_CfbA              PVFLASGVHITKDIPEILKLDP.......................................................
M_hollandica_CfbA                 PVFLASGVHITKDIPAILKLDP.......................................................
M_zhilinae_CfbA                   PVFLASGVHITKDIPAILQLDP.......................................................
M_acetivorans_CfbA                PVFLASGVHITKDIPGILSLD........................................................
M_barkeri_CfbA                    PVFLASGVHITKDIPEILSLD........................................................
M_shengliensis_CfbA               PLFLAHGVHTLKDIPARLGLED.......................................................
M_luminyensis_CfbA                PCFLASGAHLTEDIPGEIGLKA.......................................................
Ca_M_intestinalis_CfbA            PCFLASGMHLTEDIPLAIGLPI.......................................................
Ca_M_nitroreducens_CfbA           PIFLAHGVHTMEDIPQILGISR.......................................................
Ca_S_caldarius_CfbA               PVFIAKGVHTTSDITEVIAKVK.......................................................
A_fulgidus_CbiXS                  PLFISYGLHVTEDLPDLLGFPR.......................................................
G_ahangari_CbiXS                  PLFISYGLHVTEDLPDFFGFER.......................................................
S_islandicus_CbiXS                PLLFATGTHFKRDIPRLLGIDG.......................................................
A_sulfidivorans_CbiXS             PLLFAAGVHFYKDIPRLLGIN........................................................
B_subtilis_SirB                   PLLLLTAAHAKHDIPEEIVRVASRYPSVRISYGKPIGIDEEVVKAVYHRMKDIGVPYENARVVLIGRGSSDPDVKRDVTG
```

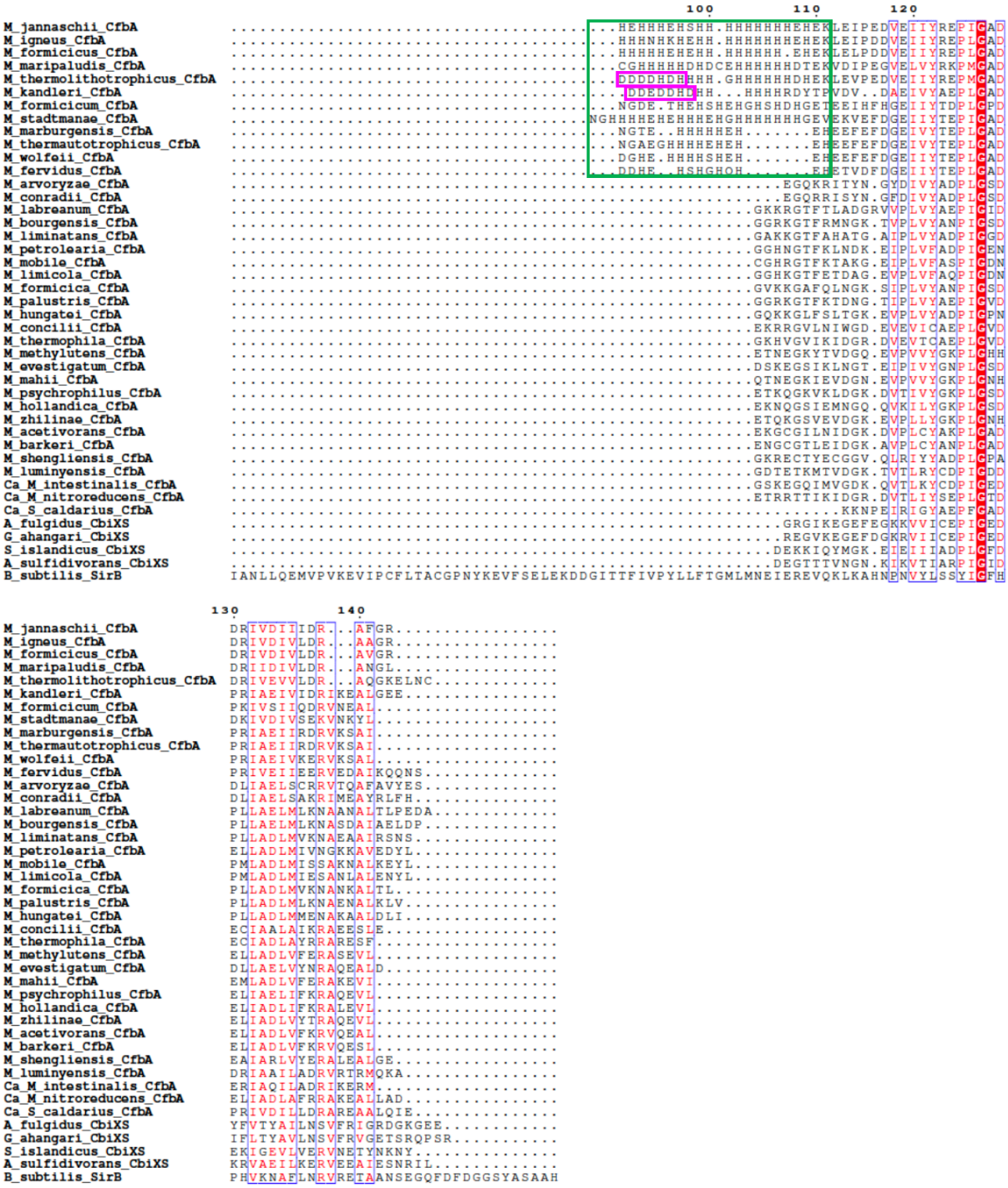

Fig. S4. Amino acid sequence alignments. Strictly conserved amino acid residues are indicated by white letters in a red shaded box. Regions containing well-conserved amino acids are indicated by red letters in a blue framed box. His-rich regions are shown in a green framed box. Asp/Glu-rich regions interspersed in His-rich regions are also shown in a pink framed box.

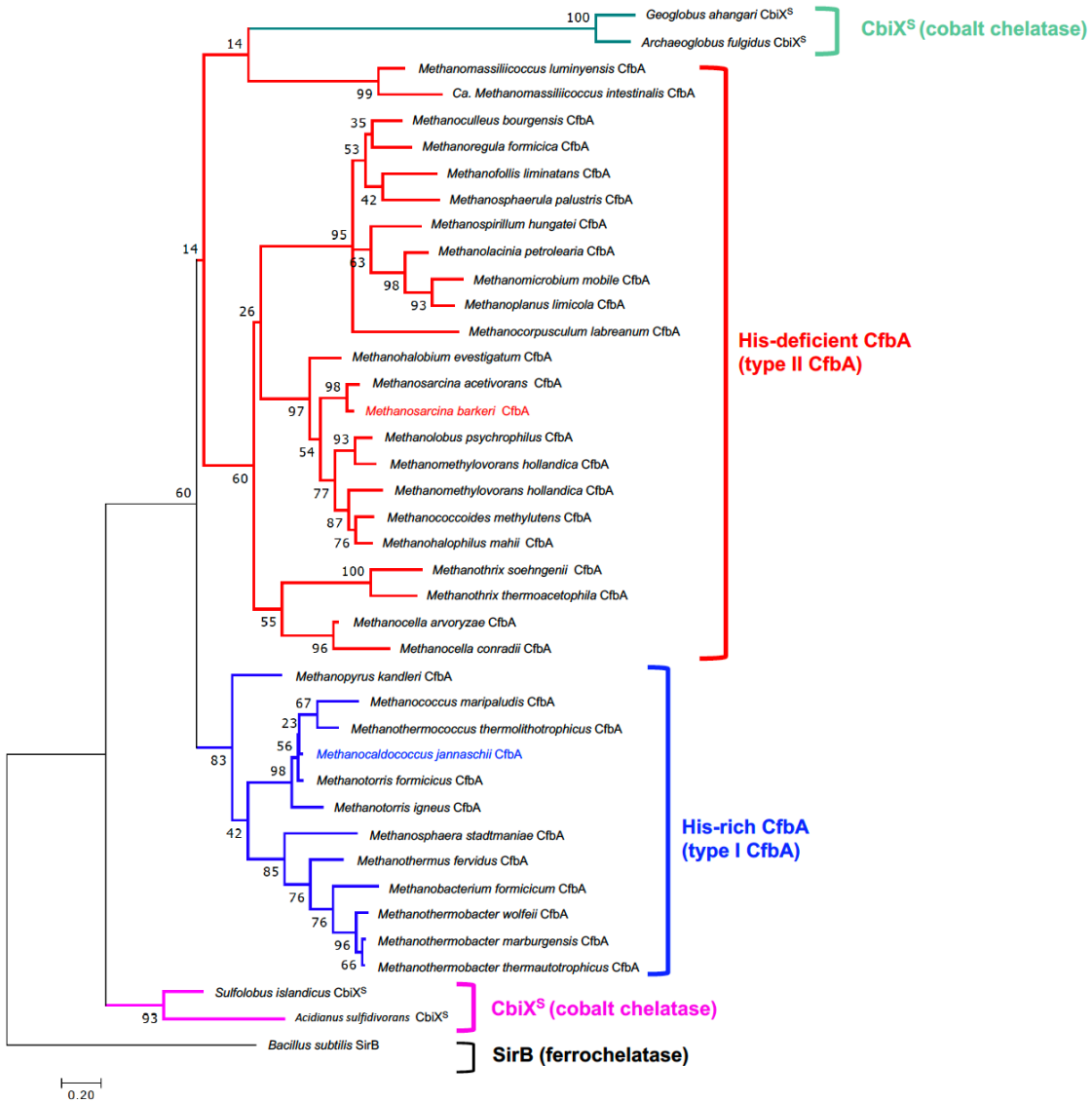

Fig. S5. Phylogenetic relationships among CfbA, CbiX^S, and SirB. The clades of type I His-rich CfbA nickel chelatases (e.g., *M. jannaschii* CfbA) and type II His-deficient CfbA nickel chelatases (e.g., *M. barkeri* CfbA) were coloured in blue and red, respectively. The clades of CbiX^S cobalt chelatases from *Sulfolobales* and *Archaeoglobales* are coloured in pink and green, respectively. The bootstrap values are indicated on each branch.

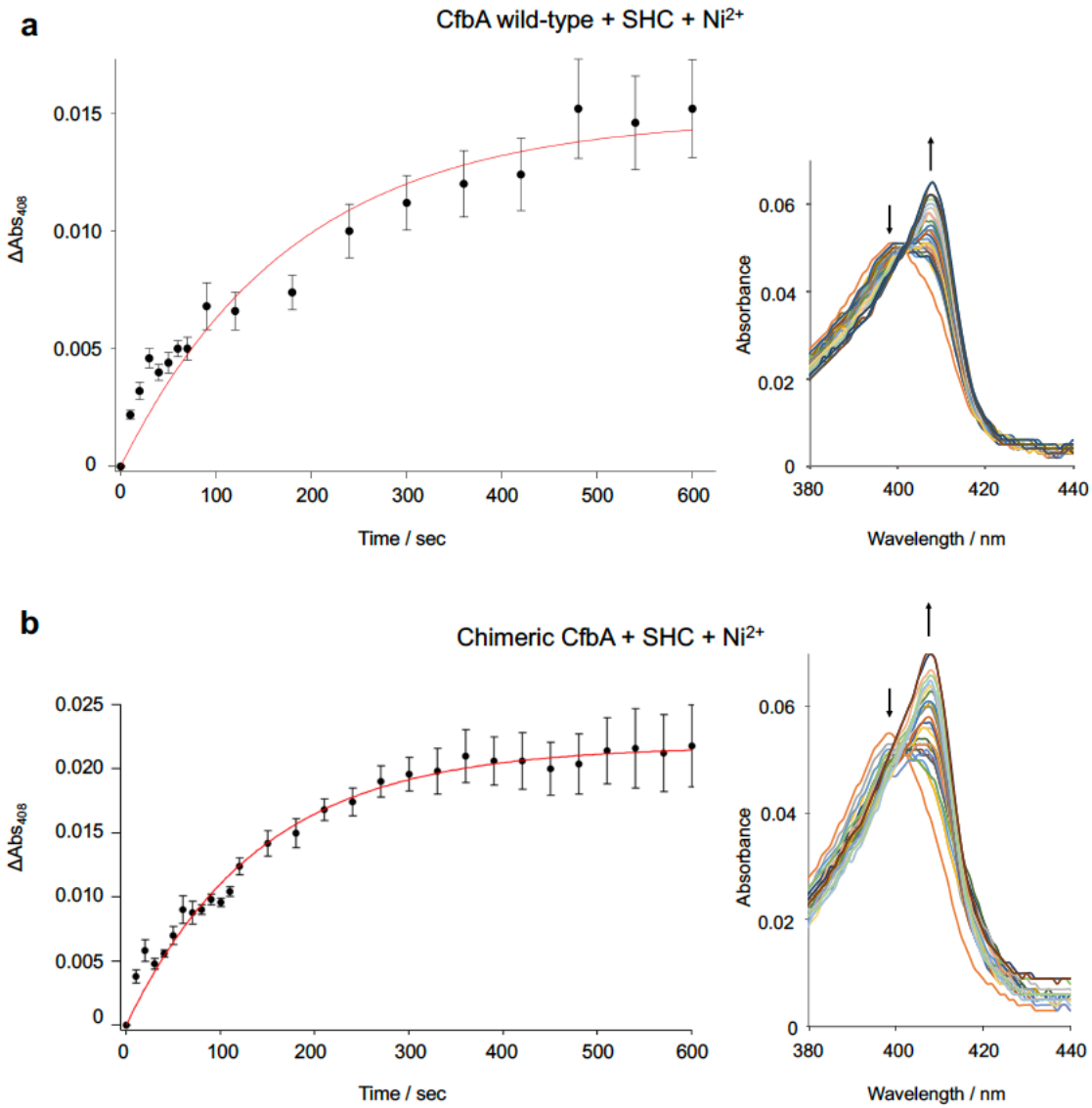

Fig. S6. The *in vitro* activity assay for Ni^{2+}-insertion into SHC. (a) Wild-type CfbA with Ni^{2+}. (b) Chimeric CfbA with Ni^{2+}. The change in absorbance over time and UV-visible spectra after the addition of Ni^{2+} or Co^{2+} to the reaction mixture was measured at 408 nm. The curves resulted from a non-linear least squares data fitting are shown as red lines for calculation of pseudo-first-order kinetic constant (k_{app}), which is described as a specific activity. The curve-fittings were calculated using Igor Pro. 8.0 software.

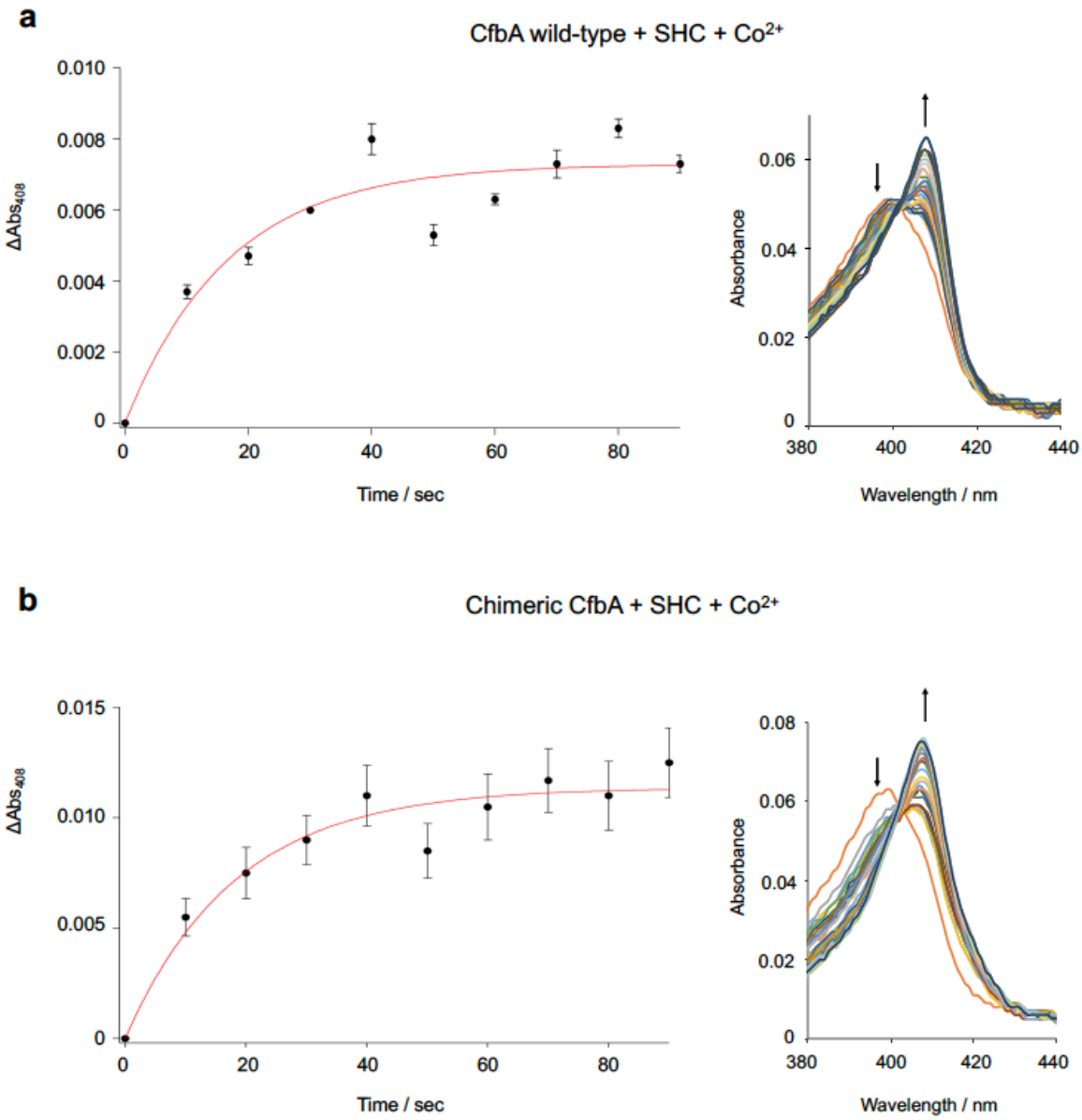

Fig. S7. The *in vitro* activity assay for Co^{2+}-insertion into SHC. (a) Wild-type CfbA with Co^{2+}. (b) Chimeric CfbA with Co^{2+}. The change in absorbance over time and UV-visible spectra after the addition of Ni^{2+} or Co^{2+} to the reaction mixture was measured at 408 nm. The curves resulted from a non-linear least squares data fitting are shown as red lines for calculation of pseudo-first-order kinetic constant (k_{app}), which is described as a specific activity. The curve-fittings were calculated using Igor Pro. 8.0 software.

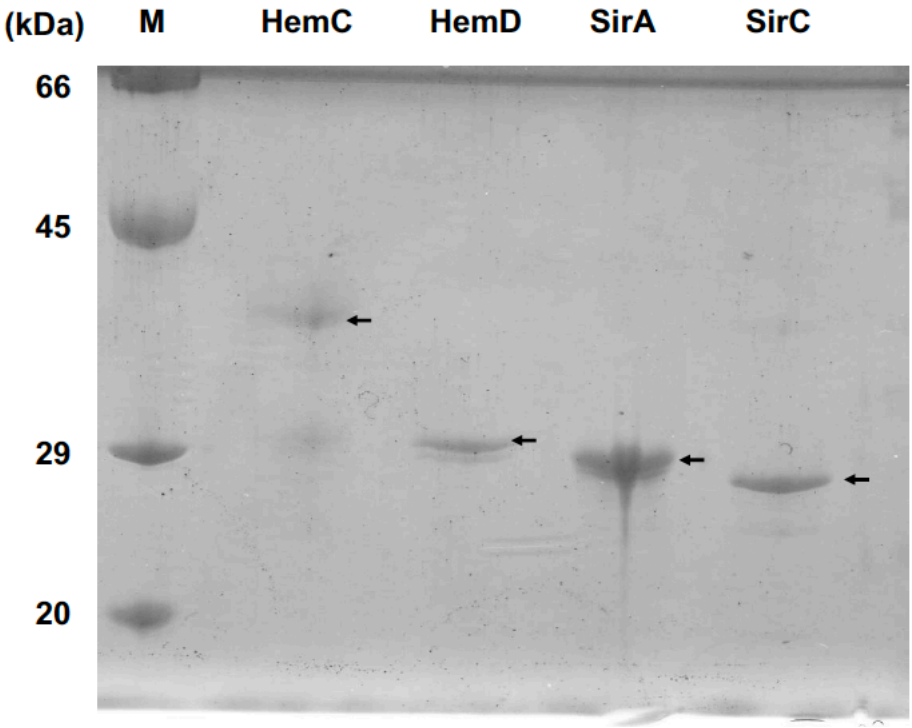

Fig. S8. SDS-PAGE analysis of HemC, HemD, SirA, and SirC. HemC, HemD, and SirA from *B. subtilis* with a C-terminal His_6-tag, and SirC from *M. barkeri* with an N-terminal His_6-tag were expressed recombinantly in *E. coli* and purified. Arrows indicate the bands corresponding to the purified proteins.

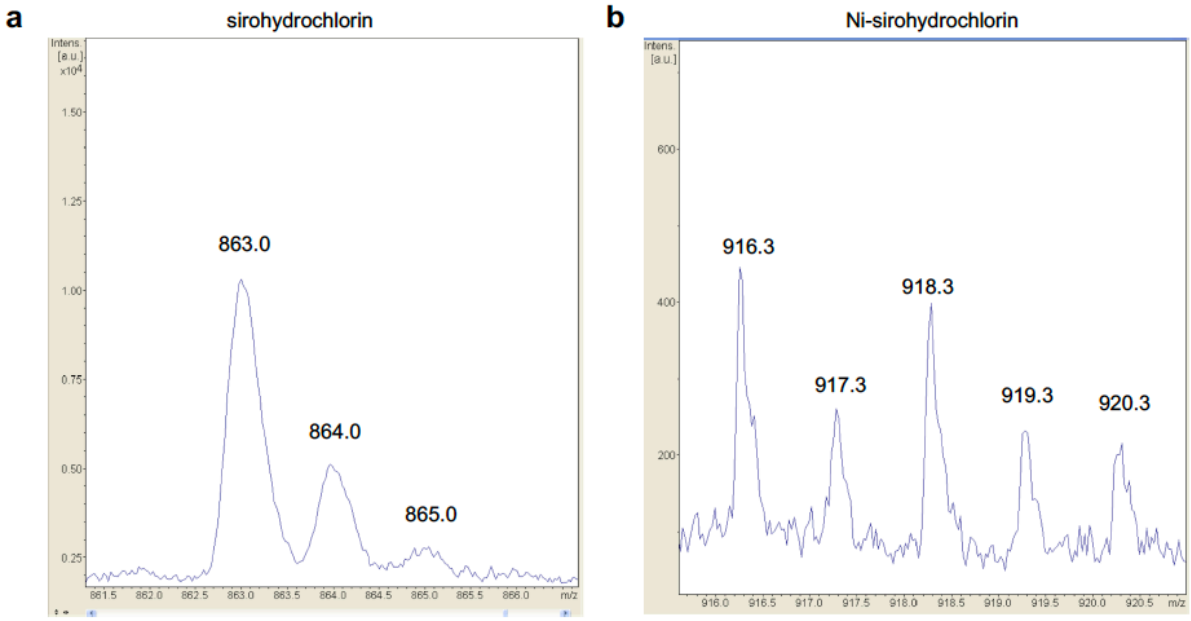

Fig. S9. MALDI-TOF/MS spectra. (a) Sirohydrochlorin (SHC). (b) nickel-sirohydrochlorin (Ni-sirohydrochlorin, Ni-SHC). The MS spectra were measured using α-cyano-4-hydroxycinnamic acid as a matrix.

Table S1. List of primers used for *M. jannaschii cfbA*.

Primer[a]	**Sequence**
NcoI_MjCfbA-F	5'-AAGGCCATGGAAGCGTTGGTTTTAGTAGGACATG-3'
SalI_MjCfbA-R	5'-CCCGTCGACTTATCTTCCAAATGCTCTATCGATAATTATATCAA-3'
NcoI_MjCfbA_H9A-F	5'-TATACCATGGAAGCGTTGGTTTTAGTAGGAGCTGGGAGTAGATTACCCTACAGCAAAG-3'
MjCfbA_E42A-F	5'-GCGTTTAGTGAGCCAACAATACCTCAAGCAG-3'
MjCfbA_E42A-R	5'-CATCAAACCAATTTCAACTATTGGGAATAAATTTCTCTC-3'
MjCfbA_H75A-F	5'-GCTACAACAAGAGATATTCCAAGGTTATTGGGG-3'
MjCfbA_H75A-R	5'-AATTCCATGAGCTAAGAAAACAGGAACAACAATG-3'
No_His_rich_MjCfbA_pCDF-F	5'-GTTGAATTATATATAGAGAACCTATTGGAGCAGATG-3'
No_His_rich_MjCfbA_pCDF-R	5'-CAACCCCAATAACCTTGGAATATCTCTTGTTG-3'
No_His_region_MbCfbA-F	5'-CCAAGGTTATTGGGGTTGGACGAAAATGGCTGTGGTAC-3'
No_His_region_MbCfbA-R	5'-CAATAGGTTCTCTATATATAATTTCAACGGTTTTTCCGTCAATTTCCAAG-3'

[a] The used restriction sites for the cloning are underlined. Codons for mutagenesis are doubly-underlined.

Table S2. List of primers used for *hem*C, *hemD*, *sirA*, and *sirC.*

Primer[a]	**Sequence**
HemC-F	5'-AAGCCATGGTGAGAACGATTAAAGTAGGTTCCAGAC-3'
HemC-R	5'-AAACTCGAGTTTTCCATCCTCGTCAAGCTCCCGTTTTA -3'
HemD-F	5'-ACGACCATGGAAAATGATTTTCCGTTGAAAGGAAAAAC -3'
HemD-R	5'-GGGCTCGAGGTCGACTATTCTCTCTTCCTCTCTTGACATGCT-3'
SirA-F	5'-ATACCATGGGGAAAGTATATATTGTAGGAG -3'
SirA-R	5'-GGGCTCGAGCAACGCCTCGCTTAAATCTTGTTTTTTTAGTTC -3'
SirC-F	5'- CCCGGATCCGCATATGGCTGAAACAAACAATTTTCTCCCGC-3'
SirC-R	5'- CCCCTCGAGGTCGACTCTACTGGAATTATCAAGGTAACCTGAAA-3'

[a] The used restriction sites for the cloning are underlined.

Table S3. Reservoir solutions for CfbA crystallization.

Crystal	Reservoir conditions
CfbA, $P4_1$ form	0.1 M ammonium sulfate, 0.3 M Na-formate, 0.1 M Tris-HCl, 3% (w/v) γ-PGA, 5% (w/v) PEG3350, pH 7.8
CfbA, $P2_12_12_1$ form	0.2 M ammonium formate, 20% (w/v) PEG3350, pH 6.6
Ni^{2+}-bound CfbA	0.1 M ammonium sulfate, 0.3 M Na-formate, 0.1 M Tris-HCl, 3% (w/v) γ-PGA, 5% (w/v) PEG3350, pH 7.8
Co^{2+}-bound CfbA	0.2 M L-arginine, 0.1 M MES-NaOH, 8% (w/v) γ-PGA, pH 6.5
Co^{2+}-and formate-bound CfbA	0.1 M ammonium sulfate, 0.3 M Na-formate, 0.1 M Tris-HCl, 3% (w/v) γ-PGA, 5% (w/v) PEG3350, pH 7.8
Chimeric CfbA	0.1 M ammonium sulfate, 0.3 M Na-formate, 0.1 M Tris-HCl, 3% (w/v) γ-PGA, 10% (w/v) PEG2000MME, pH 7.8
Sirohydrochlorin (SHC)-bound CfbA	0.1 M ammonium sulfate, 0.3 M Na-formate, 0.1 M Na-acetate, 3% (w/v) γ-PGA, 5% (w/v) PEG3350, pH 5.0
Nickel-sirohydrochlorin (Ni-SHC)-bound CfbA	0.3 M Na-malonate, 0.1 M Tris-HCl, 8% (w/v) γ-PGA, pH 7.8
Cobalt-sirohydrochlorin (Co-SHC)-bound CfbA	0.1 M ammonium sulfate, 0.3 M Na-formate, 0.1 M Na-acetate, 3% (w/v) γ-PGA, 5% (w/v) PEG3350, pH 5.0
Catalytic intermediate Ni^{2+}-SHC-His complex in CfbA	0.1 M ammonium sulfate, 0.3 M Na-formate, 0.1 M Na-acetate, 3% (w/v) γ-PGA, 5% (w/v) PEG3350, pH 5.0

Table S4. X-ray data collection and refinement statistics.

	CfbA, $P4_1$ form	CfbA, $P2_12_12_1$ form	Ni^{2+}-bound CfbA
Data collection			
Wavelength (Å)	0.980	1.486	1.486
Space group	$P4_1$	$P2_12_12_1$	$P4_1$
Resolution (Å) [a]	48.47 – 2.50 (2.59 – 2.50)	46.79 – 2.61 (2.70 – 2.61)	41.47 – 2.60 (2.69 – 2.60)
Cell dimensions			
a, *b*, *c* (Å)	68.6, 68.6, 82.4	63.4, 64.4, 69.3	68.2, 68.2, 81.2
α, *β*, *γ* (°)	90.0, 90.0, 90.0	90.0, 90.0, 90.0	90.0, 90.0, 90.0
Number of unique reflections[a]	13265 (1310)	9065 (884)	11541 (1159)
Redundancy[a]	2.0 (2.0)	24.2 (20.4)	19.3 (19.7)
Completeness (%)[a]	99.9 (99.9)	99.9 (99.9)	99.9 (100.0)
I/σ_I[a]	6.9 (2.7)	17.3 (3.2)	25.6 (4.3)
R_{merge} [a]	0.049 (0.199)	0.195 (0.962)	0.087 (1.030)
$CC_{1/2}$ [a]	0.993 (0.860)	0.998 (0.878)	0.999 (0.856)
Refinement			
Resolution (Å)	48.47 – 2.50	46.79-2.61	41.47 – 2.60
Number of reflections	13252	9063	11528
R_{work}/R_{free}[b]	0.203 / 0.244	0.196 / 0.261	0.202 / 0.240
Rmsd bond lengths (Å) [c]	0.009	0.011	0.012
Rmsd bond angles (°) [c]	1.81	2.09	2.48
Ramachandran plot			
Favored regions (%)	94.02	94.19	92.67
Allowed regions (%)	5.13	4.56	6.03
Outlier regions (%)	0.85	1.24	1.29
PDB IDs	**6M25**	**6M26**	**6M27**

[a] The values in parentheses are for the highest resolution shell. [b] R_{free} was calculated as the R_{work} for 5% of the reflections, which were not included in the refinement. [c] Rmsd, root mean square deviation.

Table S4. X-ray data collection and refinement statistics. (continued)

	Co^{2+}-bound CfbA	**Co^{2+}-bound CfbA (Co-peak data set)**	**Co^{2+}- and formate-bound CfbA**
Data collection			
Wavelength (Å)	1.741	1.606	1.606
Space group	$P4_1$	$P4_1$	$P4_1$
Resolution (Å) [a]	35.14 – 3.00 (3.11 – 3.00)	35.14 – 3.34 (3.44 – 3.34)	41.70 – 2.90 (3.00 – 2.90)
Cell dimensions			
a, *b*, *c* (Å)	68.1, 68.1, 82.1	68.1, 68.1, 82.1	68.4, 68.4, 82.5
α, *β*, *γ* (°)	90.0, 90.0, 90.0	90.0, 90.0, 90.0	90.0, 90.0, 90.0
Number of unique reflections[a]	7543 (751)	10670 (916)	8426 (842)
Redundancy[a]	26.7 (23.1)	7.0 (7.0)	4.3 (4.5)
Completeness (%)[a]	99.5 (97.3)	99.9 (100.0)	99.1 (100.0)
I/σ_I[a]	34.4 (3.8)	15.7 (2.7)	11.1 (1.4)
R_{merge} [a]	0.072 (0.942)	0.083 (0.900)	0.074 (0.905)
$CC_{1/2}$ [a]	1.000 (0.884)	0.999 (0.771)	0.997 (0.655)
Refinement			
Resolution (Å)	35.14 – 3.00		41.70 – 2.90
Number of reflections	7533		8419
R_{work}/R_{free}[b]	0.188 / 0.218		0.197 / 0.245
Rmsd bond lengths (Å) [c]	0.008		0.009
Rmsd bond angles (°) [c]	1.75		1.85
Ramachandran plot			
Favored regions (%)	91.67		94.92
Allowed regions (%)	7.89		5.08
Outlier regions (%)	0.44		0.00
PDB IDs	**6M28**		**6M29**

[a] The values in parentheses are for the highest resolution shell. [b] R_{free} was calculated as the R_{work} for 5% of the reflections, which were not included in the refinement. [c] Rmsd, root mean square deviation.

Table S4. X-ray data collection and refinement statistics. (continued)

	Chimeric CfbA	**Sirohydrochlorin (SHC)-bound CfbA**	**Nickel-sirohydrochlorin (Ni-SHC)-bound CfbA**
Data collection			
Wavelength (Å)	1.000	1.607	1.485
Space group	$P3_1$	$P4_1$	$P4_1$
Resolution (Å) [a]	50.0 – 2.23 (2.33 – 2.23)	48.89 – 2.60 (2.69 – 2.60)	41.59 – 2.40 (2.49 – 2.40)
Cell dimensions			
a, *b*, *c* (Å)	50.2, 50.2, 90.9	69.1, 69.1, 81.7	68.2, 68.2, 82.0
α, *β*, *γ* (°)	90.0, 90.0, 120.0	90.0, 90.0, 90.0	90.0, 90.0, 90.0
Number of unique reflections[a]	12499 (1552)	11899 (1175)	14774 (1486)
Redundancy[a]	9.3 (6.3)	13.7 (13.3)	13.4 (14.1)
Completeness (%)[a]	99.7 (97.8)	99.9 (100.0)	99.9 (100.0)
I/σ_I[a]	8.56 (1.7)	25.7 (2.9)	20.7 (3.7)
R_{merge} [a]	0.174 (0.846)	0.059 (0.977)	0.066 (0.771)
$CC_{1/2}$ [a]	0.997 (0.832)	0.999 (0.823)	0.999 (0.894)
Refinement			
Resolution (Å)	50.0 – 2.23	48.89 – 2.60	41.59 – 2.40
Number of reflections	12484	11889	14768
R_{work}/R_{free}[b]	0.193 / 0.235	0.187 / 0.231	0.192 / 0.227
Rmsd bond lengths (Å) [c]	0.005	0.009	0.014
Rmsd bond angles (°) [c]	1.03	1.91	2.44
Ramachandran plot			
Favored regions (%)	89.11	93.48	92.74
Allowed regions (%)	8.06	6.52	7.26
Outlier regions (%)	2.82	0.00	0.00
PDB IDs	**6M2A**	**6M2E**	**6M2F**

[a] The values in parentheses are for the highest resolution shell. [b] R_{free} was calculated as the R_{work} for 5% of the reflections, which were not included in the refinement. [c] Rmsd, root mean square deviation.

Table S4. X-ray data collection and refinement statistics. (continued)

	Cobalt-sirohydrochlorin (Co-SHC)-bound CfbA	**Catalytic intermediate Ni^{2+}-SHC-His complex in CfbA**
Data collection		
Wavelength (Å)	1.607	1.486
Space group	$P4_1$	$P4_1$
Resolution (Å) [a]	48.9 – 2.80 (2.90 – 2.80)	35.6 – 3.10 (3.21 – 3.11)
Cell dimensions		
a, *b*, *c* (Å)	69.2, 69.2, 81.8	68.9, 68.9, 83.0
α, *β*, *γ* (°)	90.0, 90.0, 90.0	90.0, 90.0, 90.0
Number of unique reflections[a]	9563 (946)	7103 (707)
Redundancy[a]	13.5 (13.9)	12.8 (13.8)
Completeness (%)[a]	99.9 (100.0)	99.6 (100.0)
I/σ_I[a]	28.3 (3.6)	16.3 (3.1)
R_{merge} [a]	0.066 (0.853)	0.117 (0.917)
$CC_{1/2}$ [a]	0.999 (0.845)	0.998 (0.830)
Refinement		
Resolution (Å)	48.9 – 2.80	35.6 – 3.10
Number of reflections	9559	7096
R_{work}/R_{free}[b]	0.184 / 0.212	0.173 / 0.212
Rmsd bond lengths (Å) [c]	0.013	0.009
Rmsd bond angles (°) [c]	2.11	1.83
Ramachandran plot		
Favored regions (%)	94.76	95.22
Allowed regions (%)	5.24	4.78
Outlier regions (%)	0.00	0.00
PDB IDs	**6M2G**	**6M2H**

[a] The values in parentheses are for the highest resolution shell. [b] R_{free} was calculated as the R_{work} for 5% of the reflections, which were not included in the refinement. [c] Rmsd, root mean square deviation.

References

1. F. Sievers and D. G. Higgins, *Protein Sci.*, 2018, **27**, 135–145.
2. X. Robert and P. Gouet, *Nucleic Acids Res.*, 2014, **42**, W320–324.
3. S. Kumar, G. Stecher and K. Tamura, *Mol. Biol. Evol.*, 2016, **33**, 1870–1874.
4. S. J. Moore, S. T. Sowa, C. Schuchardt, E. Deery, A. D. Lawrence, J. V. Ramos, S. Billig, C. Birkemeyer, P. T. Chivers, M. J. Howard, S. E. Rigby, G. Layer and M. J. Warren, *Nature*, 2017, **543**, 78–82.
5. W. Kabsch, *Acta Crystallogr. D Biol. Crystallogr.*, 2010, **66**, 125–132.
6. H. R. Powell, T. G. G. Battye, L. Kontogiannis, O. Johnson and A. G. W. Leslie, *Nature Protoc.*, 2017, **12**, 1310–1325.
7. A. Vagin and A. Teplyakov, *Acta Crystallogr. D Biol. Crystallogr.*, 2010, **66**, 22–25.
8. A. J. McCoy, *Acta Crystallogr. D Biol. Crystallogr.*, 2007, **63**, 32–41.
9. C. V. Romão, D. Ladakis, S. A. Lobo, M. A. Carrondo, A. A. Brindley, E. Deery, P. M. Matias, R. W. Pickersgill, L. M. Saraiva and M. J. Warren, *Proc. Natl. Acad. Sci. U. S. A.*, 2011, **108**, 97–102.
10. P. Emsley, B. Lohkamp, W. G. Scott and K. Cowtan, *Acta Crystallogr. D Biol. Crystallogr.*, 2010, **66**, 486–501.
11. A. A. Vagin, R. A. Steiner, A. A. Lebedev, L. Potterton, S. McNicholas, F. Long and G. N. Murshudov, *Acta Crystallogr. D Biol. Crystallogr.*, 2004, **60**, 2184–2195.
12. P. D. Adams, P. V. Afonine, G. Bunkoczi, V. B. Chen, I. W. Davis, N. Echols, J. J. Headd, L. W. Hung, G. J. Kapral, R. W. Grosse-Kunstleve, A. J. McCoy, N. W. Moriarty, R. Oeffner, R. J. Read, D. C. Richardson, J. S. Richardson, T. C. Terwilliger and P. H. Zwart, *Acta Crystallogr. D Biol. Crystallogr.*, 2010, **66**, 213–221.
13. R. A. Nicholls, *Acta Crystallogr. D Struct. Biol.*, 2017, **73**, 158–170.
14. N. W. Moriarty, R. W. Grosse-Kunstleve and P. D. Adams, *Acta Crystallogr. D Biol. Crystallogr.*, 2009, **65**, 1074–1080.
15. J. Painter and E. A. Merritt, *Acta Crystallogr. D Biol. Crystallogr.*, 2006, **62**, 439–450.
16. C. J. Williams, J. J. Headd, N. W. Moriarty, M. G. Prisant, L. L. Videau, L. N. Deis, V. Verma, D. A. Keedy, B. J. Hintze, V. B. Chen, S. Jain, S. M. Lewis, W. B. Arendall, 3rd, J. Snoeyink, P. D. Adams, S. C. Lovell, J. S. Richardson and D. C. Richardson, *Protein Sci.*, 2018, **27**, 293–315.
17. T. Fujishiro, Y. Shimada, R. Nakamura and M. Ooi, *Dalton Trans.*, 2019, **48**, 6083–6090.